



**HAL**  
open science

# Experimental Studies on the Cutting Characteristics of Hybrid CFRP/Ti Stacks

Jinyang Xu, Mohamed El Mansori

► **To cite this version:**

Jinyang Xu, Mohamed El Mansori. Experimental Studies on the Cutting Characteristics of Hybrid CFRP/Ti Stacks. *Procedia Manufacturing*, 2016, 5, pp.270-281. <10.1016/j.promfg.2016.08.024>. <hal-02416650>

**HAL Id: hal-02416650**

**<https://hal.science/hal-02416650v1>**

Submitted on 17 Dec 2019

**HAL** is a multi-disciplinary open access archive for the deposit and dissemination of scientific research documents, whether they are published or not. The documents may come from teaching and research institutions in France or abroad, or from public or private research centers.

L'archive ouverte pluridisciplinaire **HAL**, est destinée au dépôt et à la diffusion de documents scientifiques de niveau recherche, publiés ou non, émanant des établissements d'enseignement et de recherche français ou étrangers, des laboratoires publics ou privés.



HAL Authorization



# Experimental Studies on the Cutting Characteristics of Hybrid CFRP/Ti Stacks

Jinyang Xu\* and Mohamed El Mansori

MSMP – EA 7350, Arts et Métiers ParisTech, Rue Saint Dominique, BP 508,  
Châlons-en-Champagne 51006, France

[jinyang.xu@ensam.eu](mailto:jinyang.xu@ensam.eu), [mohamed.elmansori@ensam.eu](mailto:mohamed.elmansori@ensam.eu)

## Abstract

Owing to their enhanced mechanical properties and improved structural functions, the use of hybrid CFRP/Ti stacks (a sandwich of one CFRP laminate and one Ti alloy) has experienced an increasing trend in modern aerospace industry. The emergence of such composite-to-metal alliances, however, poses a series of new challenges to the manufacturing sectors for high-quality finishing of the material-made components. The key machining problems usually arise from the disparate natures of the stacked constituents (CFRP laminate and Ti alloy) and their respective poor machinability. To study the fundamental cutting characteristics of the bi-material assembly, this paper presents an experimental study concerning the machinability evaluation of the hybrid CFRP/Ti stacks. An orthogonal cutting configuration (OCC) derived from the real manufacturing operation was adopted to finalize the CFRP/Ti cutting comprehension by using the polycrystalline diamond (PCD) tipped tools. The cutting trials were performed under the reasonable cutting sequence strategy of CFRP → Ti as pointed out by most experimental studies. The key cutting responses including cutting forces, machined surface quality and tool wear mechanisms were precisely addressed *versus* the utilized cutting conditions. The experimental results highlight that a parametric combination of high cutting speeds and low feed rates often facilitates the reduction of cutting forces and induced damage extents. The basic damage modes promoted on the machined CFRP/Ti surfaces are observed to be fiber pullout, resin loss, surface cavity, deformation of feed marks and re-deposited materials. Moreover, the key wear mechanisms governing the PCD tool cutting are confirmed to be crater wear and flank wear, while the tool failure mode is edge chipping. To ensure the excellent machined surface quality, a stringent control of tool wear should be implemented when cutting hybrid CFRP/Ti stacks.

*Keywords:* Cutting characteristics, Hybrid CFRP/Ti stacks, PCD tool, Cutting forces, Machined surface quality, Tool wear mechanism.

\* Corresponding author at: MSMP – EA 7350, Arts et Métiers ParisTech, Rue Saint Dominique, BP 508, Châlons-en-Champagne 51006, France. Tel.: +33 03 26 69 91 67; fax: +33 03 26 69 91 97.  
E-mail addresses: [jinyang.xu@ensam.eu](mailto:jinyang.xu@ensam.eu), [jinyang.xu@hotmail.com](mailto:jinyang.xu@hotmail.com) (J. Xu).

# 1 Introduction

To meet the stringent dual requirements of lightweight and superior structural properties in aerospace industry, the mechanical engineers are seeking the use of multilayer stacked materials to obtain enhanced material advantages and to minimize the weaknesses of individual materials (Montoya et al., 2013, Zhang et al., 2015). In such circumstances, the hybrid CFRP/Ti stacks have thereby emerged and have been widely used to substitute standard composites and single metal alloys in various applications due to their best combination of mechanical and physical properties including high strength-to-weight ratio and outstanding corrosion/erosion resistance (Xu and El Mansori, 2015, Xu et al., 2016, Xu and El Mansori, 2016a). The hybrid CFRP/Ti stack typically exhibits a high strength-to-weight ratio with yield strength as high as 830 MPa and a density of roughly  $4 \text{ g/cm}^3$  (Park et al., 2014). Many giant aircraft manufacturers including Boeing, Airbus, Bombardier, *etc.*, are widely employing such superior multilayer materials to produce competitive skin segments, fuselages and wing connections of advanced commercial aircraft in order to deliver energy saving and improve system performance.

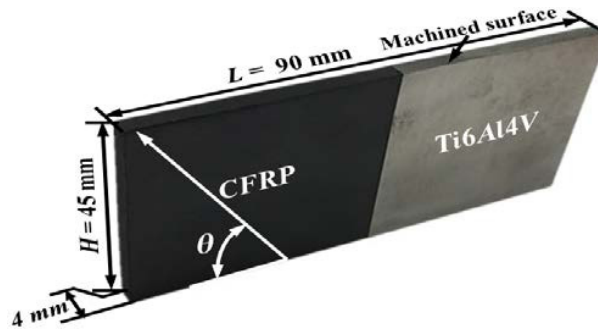
Prior to their final applications in industry, mechanical machining is frequently required for high-quality finishing of these hybrid composite structures in order to achieve dimensional accuracy and to ensure excellent assembly performance. However, machining of such composite-to-metal alliances with acceptable quality represents the most challenging task in modern manufacturing community due to the disparate machinability of the stacked constituents. The specific difficulties encountered in hybrid CFRP/Ti cutting as addressed by most experimental studies were high force/heat generation, poor machined surface quality and rapid tool wear, *etc.* (Ramulu et al., 2001, Kim and Ramulu, 2004, Park et al., 2011, Isbilir and Ghassemieh, 2013, Park et al., 2014, Kuo et al., 2014, Xu and El Mansori, 2016b). In hybrid CFRP/Ti machining, two disparate chip separation modes (brittle fracture and plastic deformation) operate throughout the entire material removal process that greatly affect the cutting behavior of the materials and subsequently the machined surface quality. For the CFRP phase machining, the composite laminate usually contains two primary constituents, *i.e.*, the reinforcing fiber and polymer matrix, exhibiting totally disparate mechanical/physical properties, making it more difficult to produce accurate part dimensions and smooth surface profiles (Xu et al., 2013, Xu et al., 2014). In addition, the highly abrasive carbon fibers bonded with the polymer matrix often cause severe abrasive wear and edge chipping of the utilized cutting tools, resulting in the excessive flank wear and short tool life (Xu et al., 2014). With respect to the Ti phase machining, the metal alloy is still regarded as one of the most difficult-to-cut materials due to its inherent high strength maintained at elevated temperature and low thermal conductivity leading to high cutting temperatures. The chips are usually produced in the nature of “serrated” shape as a result of various cycles of compression and adiabatic plastic shearing in the material removal process, causing high fluctuations of cutting force over a small chip-tool contact area (approximately 1/3 of that in the case of steels). In addition, the cutting tools employed in the Ti alloy cutting usually suffer quick diffusion wear rate and react frequently with the Ti work material due to its high chemical affinity (Nurul Amin et al., 2007). Moreover, the Ti chips can be easily welded to the tool cutting edges forming the built-up edge (BUE), which leads to premature tool failure like edge chipping (Liu et al., 2013a, Liu et al., 2013b). As such, the machining of hybrid CFRP/Ti stacks becomes more challenging and difficult than the cutting of standard composites and single Ti alloys.

To improve the machinability of the hybrid composite stacks, great attempts have been made by the worldwide scholars to study a number of cutting issues involved in the bi-material machining, *e.g.*, the machined surface quality (Ramulu et al., 2001, Kim and Ramulu, 2004, Isbilir and Ghassemieh, 2013), tool wear mechanism (Park et al., 2011, Park et al., 2012), tool performance (Isbilir and Ghassemieh, 2013, Park et al., 2014, Kuo et al., 2014). In spite of the well-covered research work, the fundamental cutting mechanisms of hybrid CFRP/Ti stacks when subjected to the most fundamental operation of orthogonal cutting still remain poorly understood. In such

circumstances, this paper aims to carry out a series of investigations concerning the key cutting characteristics of hybrid CFRP/Ti stacks based on the orthogonal cutting method by using the superior PCD tools. The main cutting responses of the bi-material assembly including cutting forces, machined surface quality, tool performance, and tool wear mechanisms were precisely addressed. A special focus was made on the investigations of the influences of tool wear progression on hybrid CFRP/Ti cutting output. The experimental studies presented in this paper can provide an enhanced cutting understanding of the multilayer stacks.

## 2 Experimental Design and Details

The investigated hybrid composite stack consisting of one annealed Ti6Al4V alloy (355 HV) and one unidirectional (UD) T300/914 CFRP laminate was provided by the VN Composites Company in France. The hybrid CFRP/Ti specimens have four basic configurations in terms of different fiber orientations ( $\theta = 0^\circ, 45^\circ, 90^\circ$  and  $135^\circ$ ) with the fixed dimensions of  $90 \text{ mm} \times 45 \text{ mm} \times 4 \text{ mm}$ . Figure 1 shows the global photograph of the used hybrid CFRP/Ti specimen. In addition, the basic mechanical/physical properties of the used hybrid CFRP/Ti stacks are summarized in Table 1.



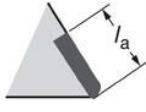
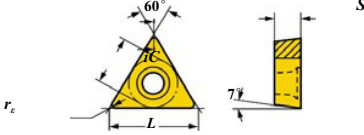


**Figure 1:** A photograph showing the basic dimensions of one hybrid CFRP/Ti stack

Workpiece material properties			
Ti6Al4V alloy		T300/914 CFRP	
Tensile strength ( $\sigma_b$ )	900-1160 MPa	Longitudinal modulus ( $E_1$ )	136.6 GPa
Elongation ( $\delta$ )	8 %	Transverse modulus ( $E_2$ )	9.6 GPa
Density ( $\rho$ )	4430 kg/m <sup>3</sup>	In-plane shear modulus ( $G_{12}$ )	5.2 GPa
Young's modulus ( $E$ )	113 GPa	Major Poisson's ratio ( $\nu_{12}$ )	0.29
Poisson's ratio ( $\nu$ )	0.342	Longitudinal tensile strength ( $X_T$ )	1500 MPa
Thermal expansion coefficient ( $\alpha_T$ )	$9.1 \times 10^{-6} \text{ } ^\circ\text{C}^{-1}$	Longitudinal compressive strength ( $X_C$ )	900 MPa
Melting temperature ( $T_m$ )	1680 °C	Transverse tensile strength ( $Y_T$ )	27 MPa
Thermal conductivity ( $\lambda$ )	7.0 W/(m·°C)	Transverse compressive strength ( $Y_C$ )	200 MPa
Specific heat ( $c_p$ )	546 J/(kg·°C)	In-plane shear strength ( $S_{12}$ )	80 MPa
—	—	Longitudinal shear strength ( $S_L$ )	80 MPa
—	—	Transverse shear strength ( $S_T$ )	60 MPa

**Table 1:** Basic mechanical/physical properties of the studied hybrid CFRP/Ti6Al4V specimen

To finalize the experimental investigations, the ISO-specified polycrystalline diamond (PCD) tipped inserts (tool reference: TCMW16T304FLP CD10) provided by Sandvik Coromant were adopted. The PCD material was welded to a tungsten carbide (WC/Co) substrate with a defined tool rake angle of  $\alpha = 0^\circ$  and a clearance angle of  $\gamma = 7^\circ$  as shown in Table 2. Besides, the PCD cutting zone was manufactured with a very small cutting radius and a quite flat surface in order to ensure a sharp cutting edge for the manufacturing operations. Figure 2 shows the optical photograph and SEM observation of the PCD tipped cutting zone.

Cutting tool						
	Tool material composition					
	Tool reference		Tipped material		Tool substrate	
	TCMW16T304FLP CD10		PCD		WC/Co	
Geometrical dimensions (mm)						
Rake angle	Clearance angle	$iC$	$S$	$r_e$	$L$	
$0^\circ$	$7^\circ$	9.525	3.96875	0.3969	16.4978	
		Effective cutting length ( $l_a$ )				
		7.4 mm				

**Table 2:** Details of the used PCD tool in orthogonal cutting of hybrid CFRP/Ti stacks

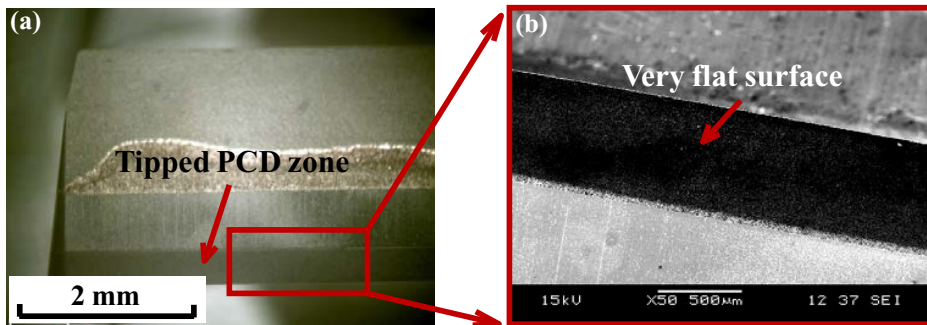


**Figure 2:** (a) Optical photograph and (b) SEM observation of the PCD tipped cutting zone

The hybrid CFRP/Ti cutting was performed subjected to the orthogonal cutting configuration (OCC) on a shaper machine tool (model GSP-EL 136) with the maximum power of 5222 W, a maximum stroke of 650 mm and a maximum speed of 100 m/min. A piezoelectric Kistler dynamometer (type 9255B) connected to a multichannel charge amplifier (type 5017B1310) and a data acquisition board was utilized to record and measure the cutting force signals during cutting. Each measurement was repeated three times in order to get reliable results. The hybrid CFRP/Ti specimen was fixed by two plate steels above the Kistler dynamometer and the cutting tool was imposed with a cutting velocity to fulfill the cutting trials. Since the CFRP phase and Ti phase exhibit different machinability behaviors, a compromise selection of the cutting parameters as summarized below: cutting speed ( $v_c = 20, 32, 50,$  and  $80$  m/min) and feed rate ( $f = 0.05, 0.10, 0.15,$  and  $0.20$  mm/rev) was adopted for the on-site tests. A schematization of the tool geometry and cutting variable definition is depicted in Figure 3, where  $F_c$  signifies the cutting force and  $F_t$  denotes the thrust force. After the completion of the cutting trials, the machined surface quality was evaluated and analyzed by using the Nikon tool maker’s SMZ-2T optical microscope and JSM-5510LV scanning electron microscope (SEM). To record the tool wear extent, the flank wear was measured

several times by using the built-in software in the Nikon SMZ-2T microscope according to the ISO Standard 3685 (1993) with average flank wear width (VB) used for carbide tools. Moreover, to facilitate the wear mechanism inspections, the SEM analyses on the worn tool surfaces were also performed.

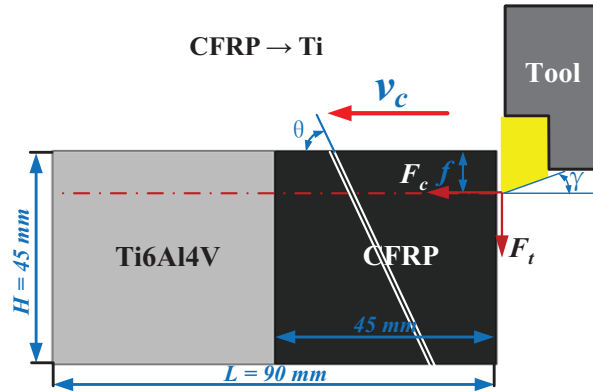


**Figure 3:** Scheme of the definitions of tool geometries and cutting variables in CFRP/Ti cutting

### 3 Results and Discussion

#### 3.1 Force Generation Analysis

In hybrid CFRP/Ti machining, two disparate types of force generation will be promoted controlling the entire chip removal process when the tool edge cuts from one phase to another phase due to the varying properties of each stacked constituent. Specifically, the forces generated in orthogonal cutting can be decomposed into two components, *i.e.*, cutting force ( $F_c$ ) and thrust force ( $F_t$ ), which signify the tribological behaviors between the tool-chip interaction and tool-work interaction, respectively. To investigate the parametric effects on hybrid CFRP/Ti cutting, a wide range of cutting variables were examined. Figure 4 depicts the influences of different cutting variables ( $v_c$ ,  $f$  and  $\theta$ ) on the magnitudes of the two force components ( $F_c$  and  $F_t$ ). In addition, the used cutting conditions in accordance with test conditions 1-8 in Figure 4 (b) were summarized as follows: test conditions 1 - 4 ( $f = 0.20$  mm/rev and  $\theta = 0^\circ$ ):  $v_c = 20, 32, 50, 80$  m/min, respectively, and test conditions 5 - 8 ( $v_c = 50$  m/min and  $\theta = 0^\circ$ ):  $f = 0.05, 0.10, 0.15, 0.20$  mm/rev, respectively.

As shown in Figure 4 (a), the fiber orientation ( $\theta$ ) was found to have significant effects on the cutting force generation of CFRP phase machining, while its influences on Ti force generation were irregular and approximately negligible. The key mechanism dominating the  $\theta$ 's influences on CFRP/Ti cutting forces can be globally attributed to the varying chip separation modes governing the CFRP phase cutting when  $\theta$  changes. In contrast, the  $\theta$ 's effect on thrust force ( $F_t$ ) of CFRP phase cutting was found to be very slight. This is because the key source of  $F_t$  often results from the bouncing-back effects of the trimmed CFRP surface fibers on tool flank face, which should have less dependence on fiber orientation ( $\theta$ ) than the chip separation process occurring on tool-chip interface that contributes mainly to the cutting force generation ( $F_c$ ). Moreover, the force results presented in Figure 4 (b) also showed that both cutting speed ( $v_c$ ) and feed rate ( $f$ ) had remarkable influences on the CFRP/Ti force generation. Specifically, the cutting speed showed a positive impact on force magnitudes at low-speed conditions, whereas it had a negative impact on force development when high speed was applied. A reasonable explanation should be that when low speeds were used,

the cutting speed would have more significant influences on tool wear than on softening the work material. As such, an increased cutting force was promoted. By contrast, when high speed was used, the influence of cutting speed on softening the work material would become a predominant factor that decreased the force generation. Furthermore, the feed rate ( $f$ ) was observed to have a totally positive impact on the force components generated when cutting hybrid CFRP/Ti stacks. This is because the feed rate ( $f$ ) signifies the uncut chip thickness in the present study and when  $f$  increases, the tool edge is required to cut off more chip volume per cutting time, which will inevitably greatly increase the cutting resistance for further chip separation and hence result in the dramatically elevated force magnitudes.

Besides, according to the force results in Figure 4, it could be deduced that there should be a sudden force variation occurring at the CFRP/Ti interface region when the tool edge cuts from CFRP phase to Ti phase. Such phenomena would inevitably lead to the severe cutting vibration and tool-work instability governing the chip removal process, which might deteriorate the machined surface quality and initiate premature tool failure like micro chipping or edge fracture.

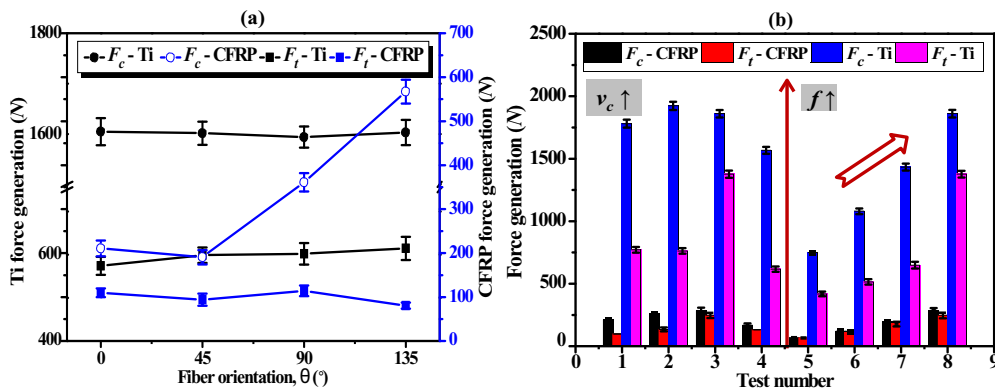


**Figure 4:** Force generation when cutting hybrid CFRP/Ti stacks in terms of (a) fiber orientation ( $\theta$ ) ( $v_c = 50$  m/min and  $f = 0.20$  mm/rev) and (b) different test conditions

### 3.2 Machined Surface Quality and Induced Damage Analyses

In hybrid CFRP/Ti cutting, the machined surface morphology plays a key role in determining the in-service performance of the material-made components and subsequently the final part acceptance. In the present study, the machined CFRP/Ti surfaces with different fiber orientations ( $\theta = 0^\circ, 45^\circ, 90^\circ, 135^\circ$ ) were examined by using both optical microscope (OM) analyses and SEM inspections. Figures 5 – 8 show the typical CFRP/Ti surfaces generated when machining with PCD tools in terms of different fiber orientations under the identical cutting conditions ( $v_c = 50$  m/min and  $f = 0.20$  mm/rev). Note that in the mentioned four figures, every three SEM observations were performed on the machined Ti phase, interface and CFRP phase, respectively, with the same magnification of  $\times 50$ .

Globally, machining of CFRP/Ti stacks with high fiber orientations (e.g.,  $\theta = 90^\circ, 135^\circ$ ) commonly produced much poorer surface quality, especially for the trimmed CFRP surfaces as depicted in Figures 7 and 8. In the mentioned two figures, a larger extent of cutting-induced fiber/matrix damage was promoted along the machined CFRP surface boundaries as compared to the cases of lower fiber orientations, e.g.,  $\theta = 0^\circ$  and  $45^\circ$ , as shown in Figures 5 and 6. The activated mechanisms controlling the varying damage formation can be attributed to the changes of the CFRP chip separation modes *versus* the fiber orientation ( $\theta$ ). Besides, the machined Ti surfaces typically were much smoother than the surfaces of the trimmed interface and CFRP phase, irrespective of the used  $\theta$  configurations. The primary damage forms of the trimmed Ti surfaces were found to be the deformation of feed marks and re-deposited chip materials. The feed marks commonly

ran toward the tool cutting direction, which occurred probably due to the plastic flow of materials during the cutting process (Zhou et al., 2003, Ezugwu et al., 2007). The re-deposited chip materials on the Ti surface were probably caused by the highly localized temperature promoted at the cutting interface that greatly facilitates the welding/adhesion process. The interface linking the CFRP phase and Ti phase was often machined with serious cracking damage due to the sudden force variations exerted on the “CFRP-to-Ti” contact boundary when the tool edge cut from CFRP phase to Ti phase. Besides, the major surface imperfections observed for the machined CFRP surface were basically fiber pullout, resin loss, and surface cavity. Further, the CFRP damage extent was also found to increase quickly when fiber orientation ( $\theta$ ) was elevated (see the comparisons among Figures 5 - 8).

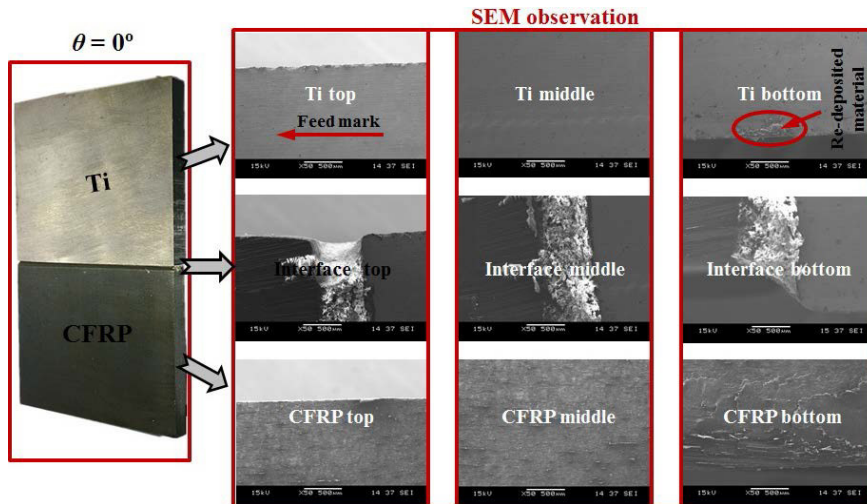


**Figure 5:** Machined CFRP/Ti surfaces with  $\theta = 0^\circ$  when cutting with PCD tools ( $v_c = 50$  m/min and  $f = 0.20$  mm/rev)

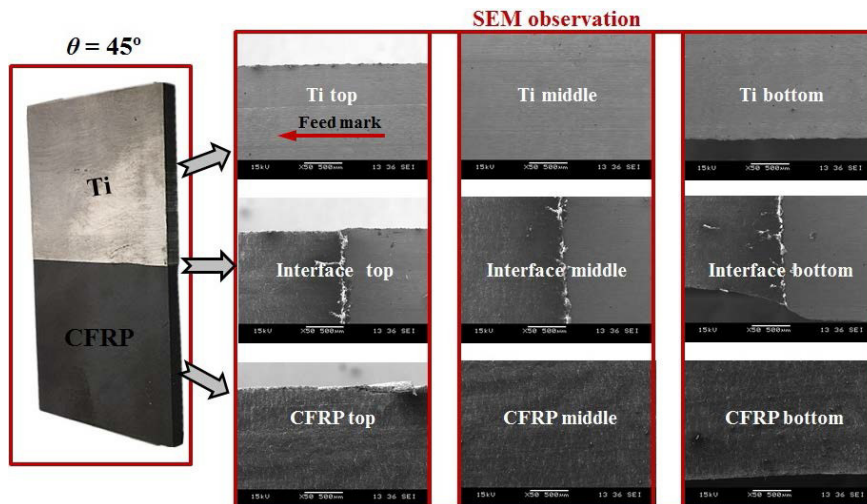


**Figure 6:** Machined CFRP/Ti surfaces with  $\theta = 45^\circ$  when cutting with PCD tools ( $v_c = 50$  m/min and  $f = 0.20$  mm/rev)

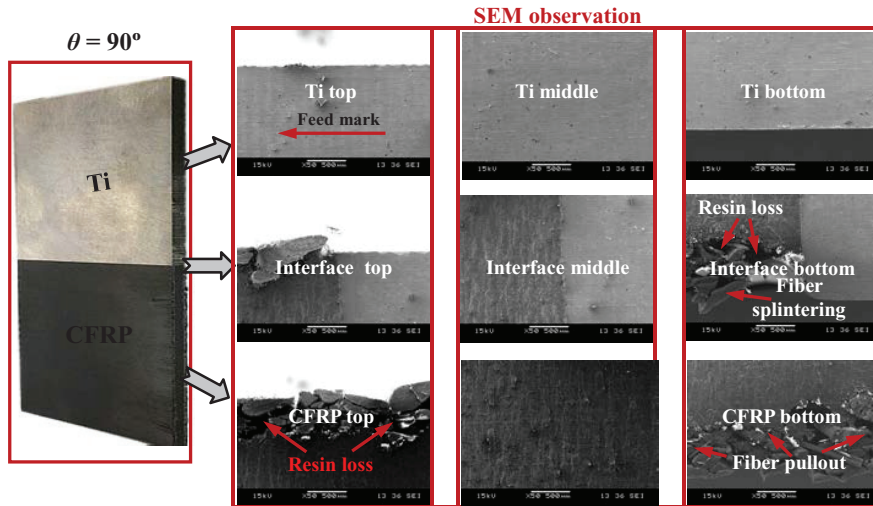


**Figure 7:** Machined CFRP/Ti surfaces with  $\theta = 90^\circ$  when cutting with PCD tools ( $v_c = 50$  m/min and  $f = 0.20$  mm/rev)

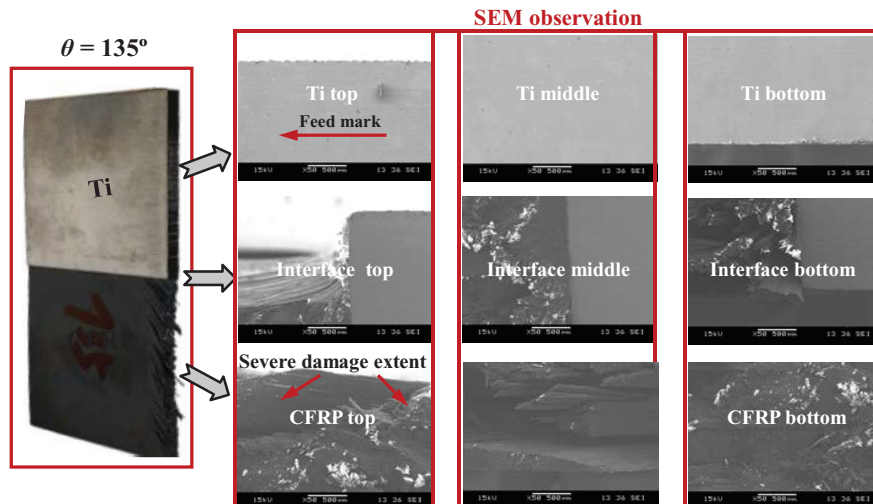


**Figure 8:** Machined CFRP/Ti surfaces with  $\theta = 135^\circ$  when cutting with PCD tools ( $v_c = 50$  m/min and  $f = 0.20$  mm/rev)

### 3.3 Tool Performance and Wear Mode Inspection

Previous research studies have confirmed the superior performance of PCD tools in CFRP composite machining due to their high hardness and high wear resistance. However, the actual performance of the PCD tools in orthogonal cutting of hybrid CFRP/Ti stacks was still not well revealed. Figure 9 then shows the tool rake and flank faces of the worn PCD tool after the completion of the orthogonal cutting trials. It could be seen that a large area of white stripe zone with approximate dimensions of  $0.51 \text{ mm} \times 4.36 \text{ mm}$ , took place on the PCD tool rake face, which referred to the serious crater wear land and signified the real tool-chip interaction area governing the entire CFRP/Ti machining. The key cause of the large cratering damage should be

primarily attributed to the Ti phase cutting during machining of hybrid composite stacks since the CFRP cutting contributes very minor effects on crater wear formation due to the insignificant or nonexistent contribution of secondary shear zone in heat generation resulting from the brittle-fracture predominant chip separation mode characterized by “dust” like chip formation as addressed by several research studies (Chang et al., 2011, Mkaddem et al., 2013). Besides, along the main cutting edge, the catastrophic failure of edge chipping was also detected on the worn PCD tool. For the occurrence of edge chipping failure, it should be owing to the sudden force variation resulting from the CFRP/Ti interface machining and also the inherent brittleness of the PCD material.

Moreover, the optical microscope analysis on tool flank face also revealed that after the completion of the cutting tests (probably after a total cutting length of 540 mm), only minor flank wear land was found along the main cutting edge, which might be attributed to the high wear resistance and high hardness of the PCD tool. Meanwhile, the edge chipping was also identified along the flank wear land through the SEM observations. The occurrence of this tool failure would greatly deteriorate the tool edge sharpness and make the tool completely lose the cutting ability.

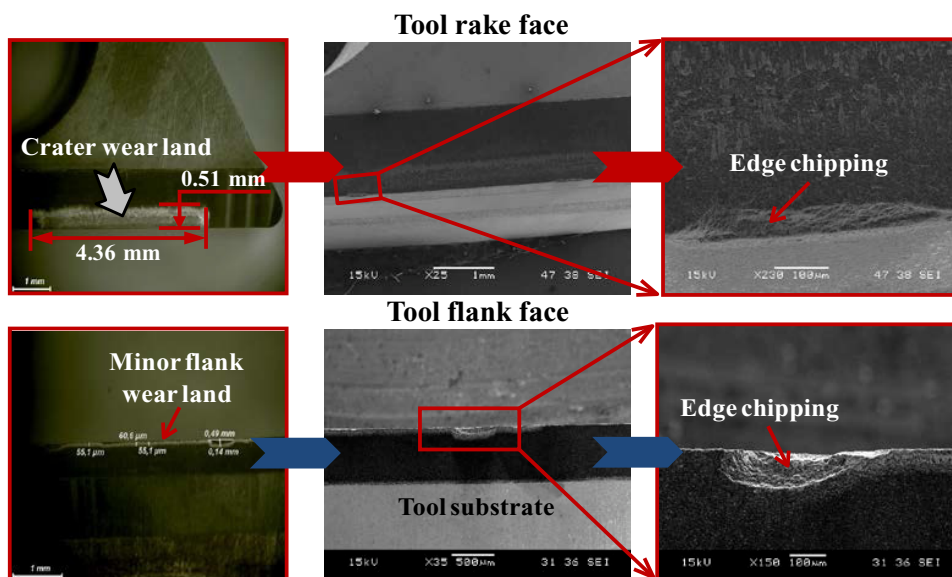


**Figure 9:** Optical micrographs and SEM observations of the PCD worn rake face and flank face after the orthogonal cutting of hybrid CFRP/Ti stacks

In addition, Figure 10 also records the influences of tool failure on the machined CFRP/Ti surface quality and the effects of tool flank wear (VB) on CFRP/Ti cutting forces. As depicted in Figure 10 (a), it was noticeable that when tool failure (edge chipping) took place on the main PCD cutting edge, the machined CFRP/Ti surface was deteriorated significantly. The severe scratching damage on the machined Ti surface was clearly visible as shown in the right photograph of Figure 10 (a). The damaged area on the machined surface may be caused due to the ineffective cutting action arising from the fractured zone of the PCD cutting edge, which causes severe scratching on the trimmed workpiece surface when it loses the fresh sharpness. Besides, the tool wear progression in terms of flank wear width (VB) was also identified to have a considerable influence on the cutting forces when machining hybrid CFRP/Ti stacks as shown in Figure 10 (b). With the progression of tool wear extents, the CFRP/Ti cutting force gradually suffered a remarkable increasing trend, especially when the VB reached to a threshold value of probably 30.53  $\mu\text{m}$ . The main cause should be due to the serious deterioration of the tool edge sharpness when the tool wear is expanded,

which inevitably gives rise to the increased tool-chip friction coefficient and subsequently leads to the high cutting resistance and high cutting energy consumption. In summary, the effects of tool failure or tool wear on hybrid CFRP/Ti cutting were entirely detrimental. To guarantee excellent machined surface quality and to minimize the high force generation, a strict control of tool wear when cutting hybrid CFRP/Ti stacks should be implemented.

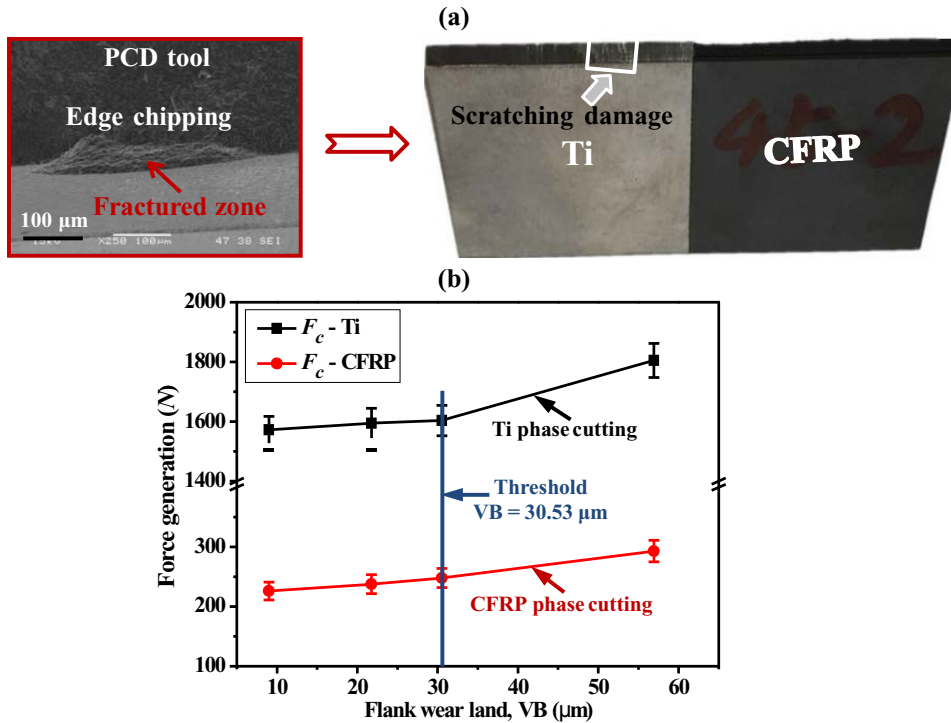


**Figure 10:** (a) Effects of tool failure on machined CFRP/Ti surface quality ( $\theta = 45^\circ$ ,  $v_c = 32$  m/min and  $f = 0.20$  mm/rev) and (b) influences of tool flank wear width (VB) on CFRP/Ti cutting forces ( $\theta = 45^\circ$ ,  $v_c = 32$  m/min, and  $f = 0.20$  mm/rev)

## 4 Conclusions

In this paper, the fundamental cutting characteristics of hybrid CFRP/Ti stacks subjected to the orthogonal cutting have been precisely investigated by utilizing the PCD tools. Based on the above experimental results, the following specific conclusions can be drawn.

- (1) Fiber orientation ( $\theta$ ) is found to have a pronounced effect on the cutting forces for the CFRP phase machining, while its influence on Ti cutting force is minor and negligible. Besides, the fiber orientation ( $\theta$ ) is observed to have minor influences on the thrust force generation for CFRP phase machining. This should be due to the fact that the key source of  $F_t$  primarily results from the bouncing-back effects of the trimmed CFRP surface fibers on tool flank face, which should have less dependence on fiber orientation ( $\theta$ ) than the chip separation process occurring on tool-chip interface that contributes mainly to the cutting force generation ( $F_c$ ). Moreover, cutting speed ( $v_c$ ) is identified to have a positive impact on CFRP/Ti force generation when low speed is used, whereas when high speed is employed,

its impact is negative. The reason can be attributed to the different extents of the cutting speed on softening work material and on tool wear progression that affect the force development. By contrast, the feed rate ( $f$ ) totally has a significantly positive impact on both cutting force and thrust force when cutting hybrid CFRP/Ti stacks.

- (2) The surface quality studies highlight that the key damage on the trimmed CFRP/Ti surfaces primarily takes place on the CFRP phase and interface. Fiber orientation ( $\theta$ ) is confirmed to have a significant role in affecting the finally machined CFRP/Ti surface quality. The key damage modes of the machined Ti surfaces are the deformation of feed marks and re-deposited chip materials, while the major imperfections on the machined CFRP surfaces are found to be fiber pullout, resin loss, and surface cavity.
- (3) Tool performance and wear analyses reveal that the PCD tools commonly suffer serious crater wear but undergo minor flank wear when orthogonal cutting hybrid CFRP/Ti stacks. The former should be attributed to the Ti phase cutting, while the latter may be due to the extremely high wear resistance of the tool material in the chip removal process. In addition, the tool failure mode for PCD tools is identified to be edge chipping due to the sudden force variation resulting from CFRP/Ti interface cutting and also the inherent brittleness of PCD.
- (4) Both tool failure and tool wear progression are confirmed to have totally detrimental influences on the machined CFRP/Ti surface quality and cutting force generation. To ensure the excellent machined surface quality, the use of freshly sharp tool and a stringent control of tool wear should be implemented when cutting stacked CFRP/Ti.

## Acknowledgments

The authors gratefully acknowledge the financial support of China Scholarship Council (CSC) (Contract No. 201306230091). The authors also thank Mr. Julien Voisin for his technical assistance in the orthogonal cutting experiments.

## References

- Chang CS, Ho JE, Chan CH and Hwang BC. Prediction of cutting temperature in turning carbon fiber reinforced plastics composites with worn tools. *Journal of Applied Sciences* 2011; 11(22): 3698-3707.
- Ezugwu EO, Bonney J, Da Silva RB and Cakir O. Surface integrity of finished turned Ti-6Al-4V alloy with PCD tools using conventional and high pressure coolant supplies. *International Journal of Machine Tools and Manufacture* 2007; 47(6): 884-891.
- Isbilir O and Ghassemieh E. Comparative study of tool life and hole quality in drilling of CFRP/titanium stack using coated carbide drill. *Machining Science and Technology* 2013; 17(3): 380-409.
- Kim D and Ramulu M. Drilling process optimization for graphite/bismaleimide-titanium alloy stacks. *Composite Structures* 2004; 63(1): 101-114.
- Kuo CL, Soo SL, Aspinwall DK, Bradley S, Thomas W, M'Saoubi R, Pearson D and Leahy W. Tool wear and hole quality when single-shot drilling of metallic-composite stacks with diamond-coated tools. *Proceedings of the Institution of Mechanical Engineers, Part B: Journal of Engineering Manufacture* 2014; 228(10): 1314-1322.
- Liu Z, An Q, Xu J, Chen M and Han S. Wear performance of (nc-AlTiN)/(a-Si<sub>3</sub>N<sub>4</sub>) coating and (nc-AlCrN)/(a-Si<sub>3</sub>N<sub>4</sub>) coating in high-speed machining of titanium alloys under dry and minimum quantity lubrication (MQL) conditions. *Wear* 2013a; 305(1-2): 249-259.

- Liu Z, Xu J, Han S and Chen M. A coupling method of response surfaces (CRSM) for cutting parameters optimization in machining titanium alloy under minimum quantity lubrication (MQL) condition. *International Journal of Precision Engineering and Manufacturing* 2013b; 14(5): 693-702.
- Mkaddem A, Ben Soussia A and El Mansori M. Wear resistance of CVD and PVD multilayer coatings when dry cutting fiber reinforced polymers (FRP). *Wear* 2013; 302(1-2): 946-954.
- Montoya M, Calamaz M, Gehin D and Girot F. Evaluation of the performance of coated and uncoated carbide tools in drilling thick CFRP/aluminium alloy stacks. *International Journal of Advanced Manufacturing Technology* 2013; 68(9-12): 2111-2120.
- Nurul Amin AKM, Ismail AF and Nor Khairusshima MK. Effectiveness of uncoated WC-Co and PCD inserts in end milling of titanium alloy-Ti-6Al-4V. *Journal of Materials Processing Technology* 2007; 192: 147-158.
- Park KH, Beal A, Kim D, Kwon P and Lantrip J. Tool wear in drilling of composite/titanium stacks using carbide and polycrystalline diamond tools. *Wear* 2011; 271(11-12): 2826-2835.
- Park KH, Beal A, Kim D, Kwon P and Lantrip J. A comparative study of carbide tools in drilling of CFRP and CFRP-Ti stacks. *Journal of Manufacturing Science and Engineering-Transactions of the ASME* 2014; 136(1): 014501.
- Park KH, Kwon P and Kim D. Wear characteristic on bam coated carbide tool in drilling of composite/titanium stack. *International Journal of Precision Engineering and Manufacturing* 2012; 13(7): 1073-1076.
- Ramulu M, Branson T and Kim D. A study on the drilling of composite and titanium stacks. *Composite Structures* 2001; 54(1): 67-77.
- Xu J, An Q, Cai X and Chen M. Drilling machinability evaluation on new developed high-strength T800S/250F CFRP laminates. *International Journal of Precision Engineering and Manufacturing* 2013; 14(10): 1687-1696.
- Xu J, An Q and Chen M. A comparative evaluation of polycrystalline diamond drills in drilling high-strength T800S/250F CFRP. *Composite Structures* 2014; 117: 71-82.
- Xu J and El Mansori M. Cutting modeling using cohesive zone concept of titanium/CFRP composite stacks. *International Journal of Precision Engineering and Manufacturing* 2015; 16(10): 2091-2100.
- Xu J and El Mansori M. Cutting modeling of hybrid CFRP/Ti composite with induced damage analysis. *Materials* 2016a; 9(1): 1-22.
- Xu J and El Mansori M. Numerical modeling of stacked composite CFRP/Ti machining under different cutting sequence strategies. *International Journal of Precision Engineering and Manufacturing* 2016b; 17(1): 99-107.
- Xu J, Mkaddem A and El Mansori M. 2016. Recent advances in drilling hybrid FRP/Ti composite: a state-of-the-art review. *Composite Structures* 2016; 135: 316-338.
- Zhang L, Liu Z, Tian W and Liao W. Experimental studies on the performance of different structure tools in drilling CFRP/Al alloy stacks. *International Journal of Advanced Manufacturing Technology* 2015; 81(1-4): 241-251.
- Zhou L, Shimizu J, Muroya A and Eda H. Material removal mechanism beyond plastic wave propagation rate. *Precision Engineering* 2003; 27(2): 109-116.